

## Smart DNA hydrogels with uncommon phase diagrams

F. BOMBOI

*Dipartimento di Fisica, Sapienza Università di Roma - Roma, Italy*

received 31 May 2018

**Summary.** — Beside its biological importance as a gene-encoding molecule, DNA plays nowadays a leading role in materials research: the newborn field of DNA nanotechnology is based on its ability to purposely self-assemble into a large variety of complex mesoscopic structures with diverse functionalities. Anyhow, the addressability of DNA self-assembly can also be exploited to produce high quantities of identical nano-sized all-DNA particles with programmable mutual interactions that can be used to test in the lab intriguing theoretical intuitions. Along this line, we have recently shown that a convenient design of competitive interactions in aqueous mixtures of monovalent and tetravalent DNA nanoparticles results in the achievement of an unconventional mechanism of gelation upon heating and of a peculiar re-entrant phase separation, demonstrating the enormous potential of DNA controlled assembly in dictating the physics of the nanoparticles response. Here, beside reviewing the main experimental results obtained by using DNA nanoconstructs, we provide insights on the aforementioned gelling by heating process, presenting additional Dynamic Light Scattering measurements performed inside the phase-separation region in order to fully characterize the dynamics of the system.

### 1. – Introduction

Since the early '80s, thanks to Seeman's brilliant intuition [1], DNA has emerged as a functional building block due to both its structural properties (nano-sized dimensions, stiffness, structural repetition) and its addressable and thermo-reversible hybridisation. After forty years, structural DNA nanotechnology is a well-established, promising field of science which makes use of purposely designed DNA patterns to realize objects with desired shapes and functionalities and complicated 2D/3D arrangements [2-5]. Such structures find applications in many fields, ranging from photonics [6] to molecular biology [7]. Building on the success of DNA nanotechnology, a parallel road has very recently been traced: the use of DNA nanoconstructs, *i.e.* self-assembling nanometric structures completely made of DNA, as model systems to experimentally test important theoretical predictions and open issues of statistical mechanics. This is because, unlike other soft systems, DNA provides the possibility to produce massive quantities of

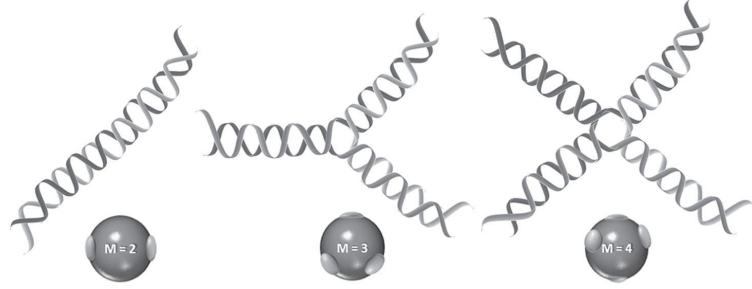


Fig. 1. – Schematic depiction of self-assembling nano-sized DNA structures. As shown, nanoconstructs can be designed on purpose to mimic colloidal particles with fixed valence  $M$ .

identical nanoparticles and to precisely dictate their features (*e.g.*, shape, coordination number, interaction strength). Figure 1 shows examples of DNA nanostructures that can be used to mimic patchy particles with restricted valence  $M$  (*i.e.*, colloidal particles that can only interact with a fixed number of nearest neighbours). Indeed, the first study in which this approach was successfully tested concerned the experimental investigation of the phase behaviour of limited-valence colloids [8]. In this work, making use of smartly designed trivalent and tetravalent DNA nanoconstructs (whose phase diagram has also been evaluated numerically [9]), the authors demonstrated the neat dependence of the phase diagram on the valence, originally predicted by theoretical and numerical studies [10]. According to these results, the progressive reduction of the maximum number of bonds that each colloidal particle can form with its nearest neighbours (*i.e.*, the particle valence) confines the gas-liquid phase separation to extremely low densities ( $\rho$ ) and temperatures ( $T$ ), thus opening a wide window in the  $T$ - $\rho$  phase diagram where the system can be cooled down to low  $T$  values without slipping into phase separation. Such finding opened intriguing scenarios such as the possibility of achieving empty liquids (liquids with extremely low density) and equilibrium gels (in which the dynamical arrest proceeds through a consecution of equilibrium states without the aid of phase separation [11, 12]) in the lab [13–16], thus confirming the huge potential of DNA nanostructures as model candidates to experimentally recreate unusual collective behaviours.

A marvelous example of this paradigm is offered by the re-entrant phase separation detected in solutions of smartly designed DNA nanoconstructs in the presence of competing thermodynamic mechanisms [17]. A brief review of this important result is reported here, conjointly with a deepening in the system dynamics through the discussion of Dynamic Light Scattering (DLS) experiments performed inside the re-entrant phase-separation region.

## 2. – Pinched phase diagram in equilibrium DNA gels

The chance of readily controlling the final shape and interaction potential of the aforementioned all-DNA structures allows for the investigation of rather complicated scenarios in which the valence of the particles may be programmed to change with the temperature. According to Thusty and Safran [18] and, more recently, to Tavares *et al.* [19] and Russo *et al.* [20], systems with a  $T$ -dependent valence exhibit a very peculiar phase diagram, characterized by a pinched phase-separation in which the coexisting dilute and dense phases accost each other at low  $T$ . A binary mixture of tetravalent ( $A$ ) and monovalent ( $B$ ) particles, originally proposed as a patchy model in [21] and experimentally

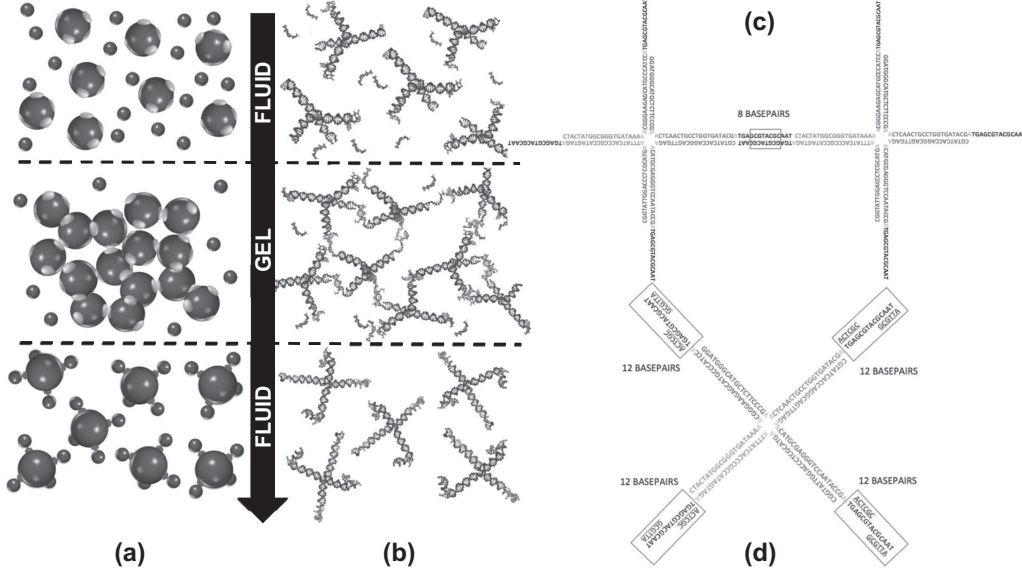


Fig. 2. – Unconventional  $T$  behaviour of the re-entrant systems and sequence design. Parallel overview of the  $T$  behaviour of binary mixtures of monovalent and tetravalent patchy particles of ref. [21](a) and of monovalent and tetravalent DNA nanoparticles of ref. [17](b). The black arrow points towards decreasing  $T$  values. In both cases, at high  $T$ , the system consists of a fluid of  $A$  and  $B$  monomers, at intermediate  $T$ ,  $A$ s bind to form a percolating network (*i.e.*, an equilibrium gel) and, at low  $T$ ,  $B$  competitors bind to the  $A$ s, displacing the  $AA$  bonds and melting the gel. (c) Scheme of two nanostars binding to form an  $AA$  bond. The black rectangle evidences the 8 base-pairs which form in a  $AA$  bond. (d) Scheme of the  $B$  competing sequences capping all the four binding sites of an  $A$  nanostar. The black rectangles evidence the 12 base-pairs which form in each  $AB$  bond.

investigated by means of DNA nanoconstructs in [17], is able to reproduce this unconventional phase behaviour if purposely designed competitive interactions are encoded in the system. In [21], the mechanism which induces the change in the system valence (and hence the pinched phase-separation) originates from the competition between two different bonding patterns: entropically favoured  $AA$  bonds (*i.e.*, bonds between the binding sites of two different  $A$  particles, which are predominant at intermediate  $T$ ) against energetically favoured  $AB$  bonds (*i.e.*, bonds between one of the four binding sites of an  $A$  particle and the one of a  $B$ , which are the stable ones at low  $T$ ). Under very strict conditions of the system composition and of the two relative interaction strengths, such competition dictates a very singular  $T$ -behaviour which is illustrated in fig. 2(a). At high  $T$  the system behaves as a fluid of non-interacting  $A$  and  $B$  particles, at intermediate  $T$  as a spanning network of bonded  $A$ 's and, at low  $T$ , as a solution of freely-diffusing clusters in which each tetravalent  $A$  particle is saturated by four monovalent  $B$ 's. The experimental transposition [17] makes use of limited-valence DNA nanostructures to recreate in the lab this unusual collective behaviour (fig. 2(b)).

Specifically, four DNA sequences are designed to self-assemble at high  $T$  into nano-sized star structures ( $A$  particles) consisting of four double-helical arms (of 20 base-pairs) each one terminating with a palindromic single-stranded sequence of 8 bases (sticky end) which furnishes inter-particle bonding via base pairing (each star can thus be considered

as a particle with  $M = 4$ , being able to bind other four analogous stars by means of its sticky overhangs). By slowly cooling the system, the tetravalent nanostars bind one to the other through the sticky terminals ( $AA$  bonds) and, at intermediate  $T$ , they form an entropically favourable network of bonded  $A$  particles, *i.e.* a low-valence equilibrium gel. An example of an  $AA$  bond is depicted in fig. 2(c): as it can be seen, when two  $A$ s bind, 8 base-pairs form. On further cooling, monovalent  $B$  particles (consisting of two distinct single stranded 6-base-long DNA sequences, designed to compete for bonding with the  $A$  particles at low  $T$ ) start binding preferentially to the  $A$  sticky ends ( $AB$  bonds), displacing the  $AA$  bonds and thus disrupting the network. Figure 2(d) shows a DNA nanostar whose sticky ends are all saturated by  $B$  competitors. When an  $AB$  bond forms, 12 couples of bases pair, thus leading to an energetically more favourable arrangement for the system. Indeed, in order to be stable at low  $T$  values,  $AB$  bonds must be energetically more favourable than the  $AA$  ones but, simultaneously, entropically more costly (in order to be activated only at low  $T$  values). This condition is implemented by splitting the  $B$  competitors into two different single-stranded sequences: this raises the entropic cost of forming  $AB$  bonds (favouring the  $AA$  ones at intermediate  $T$ ) and, at the same time, eliminates the unwanted possibility of forming  $BB$  bonds (a single  $B$  sequence should necessarily be self-complementary to bind to the palindromic nanostar sticky end).

It is worth noting that the ratio between the  $B$  competitors and the  $A$  particles is always fixed to 4, so that, at low  $T$ , there are no free competitors in solution. Conversely, as fig. 2b shows, unhybridised competitors are freely-diffusing at larger  $T$  values. Therefore, the overall valence of the system varies from four at high  $T$  (where each nanostar has four arms available to form the gel) to zero at low  $T$  (where the  $B$  competitors saturate all the possible binding sites of the tetravalent  $A$ s). As a result, the system displays the Safran like re-entrant phase diagram reported in fig. 3 [17].

To obtain this phase diagram, six DNA samples at increasing nanostar concentrations

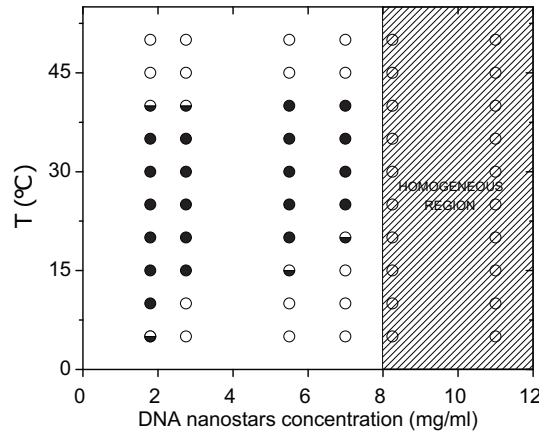


Fig. 3. – Pinched phase diagram for aqueous solutions of monovalent and tetravalent DNA nanoconstructs ( $[\text{Na}^+] = 130 \text{ mM}$ ). Open circles indicate homogeneous solutions, filled circles indicate phase separated samples and semi-filled circles indicate borderline cases. The dashed area qualitatively shows the homogeneous region where no phase-separation was detected. Data from ref. [17].

have been marked with ethidium bromide (EtBr) and photographed at various  $T$ s under UV exposition in order to investigate the  $T$ -dependence of the eventual meniscus of phase-separation inside the solutions (see ref. [17] for experimental details).

As the results show, the re-entrant phase-separation is confined to rather low nanostar concentrations: denser samples do not display coexisting phases at any  $T$ . It is worth noting that this low-density phase-separation is a distinctive feature of empty liquids which, as in the present case, are composed by particles with low coordination numbers.

### 3. – Experimental section: dynamics inside the phase-separation region

Beside giving rise to the pinched phase diagram above described, the programmed temperature behaviour of the all-DNA system (*i.e.*, separate nanostars at high  $T$ , bonded ones at intermediate  $T$  and isolated clusters at low  $T$ ) has a net effect on the dynamics. Thanks to the presence of the wide homogeneous region (dashed region in fig. 3), such dynamics has been widely investigated by means of DLS experiments on non-separating samples. Results from ref. [17] suggest that, upon cooling from high  $T$ 's, the system exhibits a continuous and fully thermo-reversible crossover from fluid to gel to fluid again. This is reflected by the intermediate scattering functions which are all characterized by a two step relaxation with the appearance of a plateau whose amplitude initially grows on cooling (as in all gel-forming systems) and then starts to decrease when  $T$  is lowered enough. The insurgence of the plateau has indeed been attributed to the progressive formation of the network of bonded  $A$  nanostars (gel) while its low- $T$  disappearance to the gradual disruption of the network due to the hybridisation of the  $B$  competing sequences, which give rise to a fluid of non-interacting, freely diffusing  $AB_4$  clusters. Here, to complete the dynamical characterization of the system, we report additional DLS measurements performed instead on a phase-separating sample, *i.e.* on a sample having a nanostar concentration ( $c = 5.5$  mg/ml) which falls inside the region of thermodynamics instability. All the measurements are carried out by focussing the laser spot below the meniscus of phase-separation in order to monitor the dynamics in the dense phase.

**3.1. Materials and sample preparation.** – The nanostar-forming oligomers were purchased from Integrated DNA Technologies (IDT) with PAGE purification. The nano-sized star structures were assembled by mixing equimolar quantities of the four sequences:

- 1) CTACTATGGCGGGTGATAAAAACGGGAAGAGCATGCCCATCCA TGA GCGTACGC AAT,
- 2) GGATGGGCATGCTCTTCCCGAACTCAACTGCCTGGTGATACGA TGA GCGTACGC AAT,
- 3) CGTATCACCAGGCAGTTGAGAACATGCGAGGGTCCAATACCGA TGA GCGTACGC AAT,
- 4) CGGTATTGGACCCTCGCATGAATTTATCACCCGCCATAGTAGA TGA GCGTACGC AAT.

Two six-base-long single-stranded DNA sequences (competitors), purchased from Integrated DNA Technologies (IDT) with standard desalting purification, were added to the nanostar solution:

- 1) ATTGCG,
- 2) CGCTCA.

The sample was reconstituted in a filtered  $H_2O$ -NaCl solution ( $[Na^+] = 130$  mM) at a final nanostar concentration of 5.5 mg/ml (*i.e.*, 0.078 mM). The ratio between the molar

concentration of each competitor and of the nanostars was set to four. The sample was then heated to 90 °C, incubated for 20 min and slowly cooled down to room temperature overnight. For DLS experiments, 40  $\mu$ l of solution were loaded into a glass capillary (Hilgenberg, inner diameter 2.4 mm), topped with 20  $\mu$ l of silicon oil and flame sealed to avoid evaporation.

**3.2. Methods.** – DLS experiments were carried out on a light scattering setup optimized to hold microlitre-sized capillaries and endowed with a 633 nm He-Ne laser (Newport, 17 mW). The scattering angle was set to 90°. A Brookhaven correlator furnishes the autocorrelation function of the scattering intensity  $g_2(t)$  which is converted into the autocorrelation function of the electric fields  $g_1(t)$  by means of the Siegert relation. The sample was initially thermalized at 55 °C for 30 min and then slowly cooled down in steps, always equilibrating it for 30 min before starting the measure. For each  $T$ , measurements lasted 15 min. All the experiments were performed by focussing the laser spot below the meniscus of phase-separation in order to study the dynamics in the dense phase (samples marked with EtBr were used as a reference to localize the meniscus level at different DNA concentrations, as indicated in [17]).

**3.3. DLS results.** – DLS measurements in the dense phase confirm the re-entrant behaviour previously observed in the homogeneous region [17]. Upon cooling from high  $T$ , the autocorrelation functions of the scattered fields evidence the progressive formation of a second (slow) relaxation whose characteristic time drastically increases as the  $T$  is lowered. Hence, even in the dense phase, we assist to a gradual slowing down of the dynamics which proceeds till approximately 30 °C (fig. 4(a)). In a previous work [13], the characteristic time of the slow relaxation in DNA hydrogel samples has been shown to correlate with the bulk viscosity of the system. Therefore, according to this interpretation, the present data suggest that the sample viscosity increases as the  $T$  is lowered from high values, marking a crossover from a low-viscous homogeneous solution to a highly viscous dense phase. Anyhow, below 30 °C (fig. 4(b)), the trend starts to invert: the autocorrelation functions become faster and faster on cooling and the second relaxation progressively disappears. Such behaviour continues even below 20 °C, *i.e.* in the region of the pinched phase diagram in which the sample comes back to homogeneous.

Therefore, even at DNA concentrations which fall inside the phase-separation region, the dynamics of the system reflects its uncommon  $T$  behaviour: the high- $T$  homogeneous state is characterized by isolated nanostars which are free to diffuse while, at intermediate  $T$ , the system undergoes a phase-separation and, in the denser phase, we observe a progressive increase of the sample viscosity likely due to the progressive formation of bonds between different nanostars (reflected by the insurgence of a plateau of increasing height in the autocorrelation functions). Eventually, at low  $T$ , the competitors start to bind to the nanostars (saturating all their possible bonding possibilities), leading to final low- $T$  liquid state made of non-interacting  $AB_4$  clusters.

#### 4. – Conclusions

Thanks to their versatility, DNA nanoconstructs are ideal systems to verify in the laboratory theoretical conjectures which can give rise to very uncommon collective behaviours. Further to demonstrate the dependence of the phase-behaviour of colloidal particles on their valence and, hence, the possibility of experimentally realizing equilibrium gels and empty liquids, DNA nanostructures have been used to recreate in the

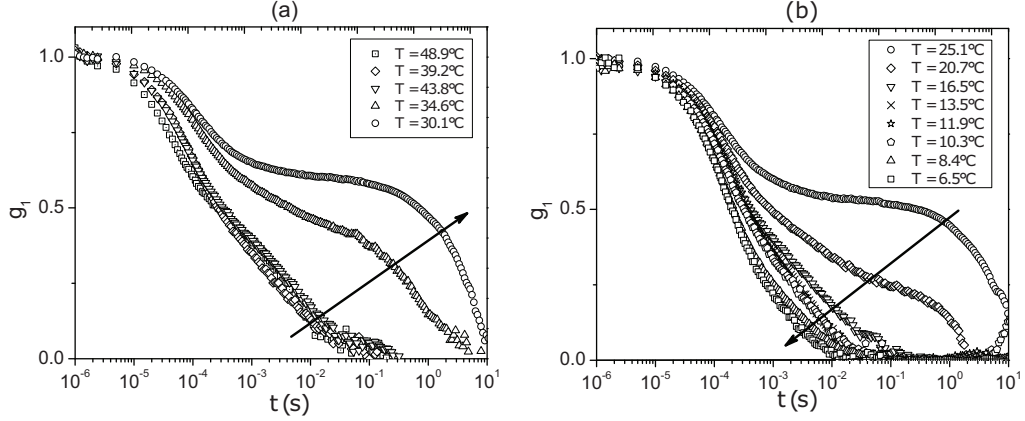


Fig. 4. –  $T$ -dependence of the autocorrelation functions of the scattered fields for a phase-separating sample ( $c_{\text{nanostar}} = 5.5 \text{ mg/ml}$ ). (a) Dynamic evolution of the system as  $T$  is lowered from roughly  $50^\circ\text{C}$  to  $30^\circ\text{C}$ . (b) Dynamic evolution of the system as  $T$  is lowered from roughly  $25^\circ\text{C}$  to  $6^\circ\text{C}$ . The black arrows point in the direction of decreasing  $T$ .

lab  $T$ -dependent valence systems whose phase diagrams are characterized by a peculiar re-entrant shape.

Specifically, solutions of monovalent and tetravalent DNA nanoparticles have been proved to undergo, in aqueous solutions, a re-entrant phase separation and a thermo-reversible gelling process which takes place even upon heating, if smartly designed competitive interactions are implemented in the system [17].

Beside reviewing this important result, we have here investigated the dynamics inside the phase-separated region, in order to complete the dynamical characterization of the system. The presented results corroborate the ones previously obtained in the homogeneous region [17], confirming the re-entrant slowing down of the dynamics and the continuous crossover from a high- $T$  low-viscosity fluid to a viscous dense phase and back to a low-viscosity homogeneous fluid at room  $T$ .

Further to demonstrate the exquisite control over the particles collective behaviours that DNA controlled assembly effectively provides, these studies are relevant for all the possible applications that biocompatible body temperature gels (behaving as liquids at ambient  $T$ ) may implicate, especially for biomedical and diagnostic purposes. Indeed, it is worth noting that the exploitation of hydrogels for bioapplications is currently the focus of an increasing number of researches [22-24].

Finally, the chance of finely tuning the DNA nanoparticles interactions, conjointly with the possibility of creating bulk quantities of identical nanoconstructs having tailored shapes and nanoscale features, opens countless scenarios such as the possibility of experimentally realizing biocompatible DNA-based thermoplastic materials (vitrimers) with self-healing and stress-releasing properties [25,26], which has been already foreseen in numerical works [27].

\* \* \*

I acknowledge all the participants to the present research: F. Romano for designing the re-entrant DNA sequences and for the theoretical evaluations of the bonding free energies, M. Leo for helping with the sample preparation and with the determination of the phase diagram, J. Fernandez-Castanon for helping with DLS experiments and data



analysis, T. Bellini, R. Cerbino, F. Bordi and P. Filetici for the precious experimental support with DNA nanostars samples, DLS setup optimization and for all the useful discussions and comments. Finally, I thank F. Sciortino for coordinating the whole work.

## REFERENCES

- [1] SEEMAN N. C., *J. Theor. Biol.*, **99** (1982) 237.
- [2] SEEMAN N. C., *Nature*, **421** (2003) 427.
- [3] CONDON A., *Nat. Rev. Genet.*, **7** (2006) 565.
- [4] PINHEIRO A. V. *et al.*, *Nat. Nanotechnol.*, **6** (2011) 763.
- [5] WEI B., DAI M. and YIN P., *Nature*, **485** (2012) 623.
- [6] SU W. *et al.*, *Angew. Chem. Int. Ed.*, **50** (2011) 2712.
- [7] YIN P. *et al.*, *Nature*, **451** (2008) 318.
- [8] BIFFI S. *et al.*, *Proc. Natl. Acad. Sci. USA*, **110** (2013) 15633.
- [9] ROVIGATTI L., BOMBOI F. and SCIORTINO F., *J. Chem. Phys.*, **140** (2014) 154903.
- [10] BIANCHI E. *et al.*, *Phys. Rev. Lett.*, **97** (2006) 168301.
- [11] ZACCARELLI E., *J. Phys. Condens. Matter*, **19** (2007) 323101.
- [12] SCIORTINO F. and ZACCARELLI E., *Curr. Opin. Colloid Interface Sci.*, **30** (2017) 90.
- [13] BIFFI S. *et al.*, *Soft Matter*, **11** (2015) 3132.
- [14] BOMBOI F. *et al.*, *Eur. Phys. J. E*, **38** (2015) 1.
- [15] FERNANDEZ-CASTANON J. *et al.*, *J. Chem. Phys.*, **145** (2016) 084910.
- [16] FERNANDEZ-CASTANON J., BOMBOI F. and SCIORTINO F., *J. Chem. Phys.*, **148** (2018) 025103.
- [17] BOMBOI F. *et al.*, *Nat. Commun.*, **7** (2016) 13191.
- [18] TLUSTY T. and SAFRAN S., *Science*, **290** (2000) 1328.
- [19] TAVARES J., TEIXEIRA P. and DA GAMA M. T., *Mol. Phys.*, **107** (2009) 453.
- [20] RUSSO J. *et al.*, *Phys. Rev. Lett.*, **106** (2011) 085703.
- [21] ROLDAN-VARGAS S. *et al.*, *Sci. Rep.*, **3** (2013) 2451.
- [22] SINGH A. and PEPPAS N. A., *Adv. Mater.*, **26** (2014) 6530.
- [23] HUEBSCH N. *et al.*, *Nat. Mater.*, **14** (2015) 1269.
- [24] GOINDI S., NARULA M. and KALRA A., *AAPS PharmSciTech*, **17** (2016) 597.
- [25] MONTARNAL M. *et al.*, *Science*, **334** (2011) 965.
- [26] DENISSEN J., WINNE M. and DU PREZ F. E., *Chem. Sci.*, **7** (2016) 30.
- [27] ROMANO F. and SCIORTINO F., *Phys. Rev. Lett.*, **114** (2015) 078104.